Metamaterial-Inspired, Electrically Small Huygens Sources

Peng Jin, *Student Member, IEEE*, and Richard W. Ziolkowski, *Fellow, IEEE*

***Abstract*—Electrically small electric and magnetic dipole antennas are introduced that are based on electric and magnetic near-field resonant parasitic (NFRP) elements that are electrically coupled to the driven element. By properly combining these two NFRP antenna types, electrically small Huygens sources are realized. The proposed Huygens sources have one feed point, are well matched to 50 Ω, and have high radiation efficiencies. Their predicted directivity patterns approach the known Huygens source theoretical limit.**

***Index Terms*—Directivity, electrically small antennas (ESAs), Huygens source.**

I. Introduction

ELECTRICALLY small antennas (ESAs) continue to be of great interest to the commercial and government sectors. A tremendous amount of work has been expended on ESA designs over the last half-century. In recent works [1], [2], studies of the efficiency, matching, bandwidth, and Q value of ESAs was emphasized. The directivity of such ESAs has been of less concern because they radiate in their fundamental dipole mode, which means their directivity is typically about 1.76 dB if they radiate in free space or 4.77 dB if they radiate appropriately in the presence of an infinite ground plane.

High directivity in and near the electrically small regime has been studied recently, both theoretically and experimentally [3]–[6]. It was noted in [5] that a single Huygens source can achieve a directivity of 4.77 dB, and a dual Huygens source should be able to achieve a directivity of 9.0 dB. An antenna with a higher directivity than is available from a simple dipole antenna in an electrically small size would be very attractive. Consequently, we have considered how to achieve an electrically small Huygens source using the recently introduced metamaterial-inspired near-field resonant parasitic paradigm [2], [7], [8].

Theoretically, a Huygens source is a particular combination of electrical and magnetic dipole antennas. They are taken to be at the same location and with the same radiation intensity, but with orthogonal polarizations [9]. A recent effort to implement an electrically small Huygens source [10] was reportedly only partially successful. It considered a combination of separately fed, low Q, spherical electric [1] and magnetic [11] dipoles. The resulting design was poorly matched to a 50-Ω source and exhibited a high Q value. Nonetheless, the directivity gains suggested in [5] were demonstrated numerically for both the single- and two-element Huygens sources.

In this letter, we propose the use of planar electrically small electric and magnetic dipoles to construct electrically small Huygens sources that are nearly completely matched to a 50-Ω source, have a high radiation efficiency, and have directivities that approach their theoretical maximum. Simulation results will be presented; they were obtained with the finite-element-based Ansoft High Frequency Structure Simulator (HFSS). In contrast to previously reported designs [10], the proposed Huygens sources have only one feed point. The letter is arranged as follows. In Section II, the electrically small electric and magnetic dipoles will be introduced. Both planar and three-dimensional (3D) Huygens source designs are proposed in Section III, along with their simulated performance characteristics. Section IV concludes this letter.

II. Electric and Magnetic Dipoles

An electrically small combination of electric and magnetic dipole antennas is needed to construct an electrically small Huygens source. In [2] and [12], metamaterial-inspired electrically small monopole antennas were introduced that had high radiation efficiencies and were nearly completely matched to a 50-Ω source. Despite their higher quality factors Q, when compared to related 3D designs, planar designs are adopted for the Huygens sources reported in this letter. With such a planar design, the phase centers of the electric dipole and magnetic dipole can be placed in very close proximity to each other. This is highly desirable in any Huygens source implementation.

Based on those monopoles designs, an electrically small electric dipole was developed. Its structure is shown in Fig. 1(a). The near-field resonant parasitic (NFRP) element (object in front) is a dipole augmented with symmetric top and bottom loadings; the source (object in back) is a variation of a center-fed top-hat dipole. The excited dipole and the NFRP element have essentially the same shape and are electrically coupled. This is a 2-oz (0.07 mm thick copper), 31-mil (0.787 mm thick substrate) Rogers Duroid 5880 board material ($\epsilon_r = 2.2$, $\mu_r = 1.0$, $\text{loss tangent} = 0.0009$) design; the driven and NFRP dipoles lie on opposite sides of one Duroid sheet. The outer radii of the driven dipole antenna and the electric NFRP element are 13.0 and 15.0 mm, respectively. Their top arcs are respectively 0.5 and 2.0 mm wide. Their gaps are respectively 22.4 and 6.4 mm

Manuscript received April 12, 2010; revised May 18, 2010 and May 20, 2010; accepted May 20, 2010. Date of publication May 27, 2010; date of current version June 10, 2010. This work was supported in part by DARPA Contract number HR0011-05-C-0068 and by ONR Contract number H940030920902.

The authors are with the Department of Electrical and Computer Engineering, University of Arizona, Tucson, AZ 85721 USA (e-mail: pjin@ece.arizona.edu; ziolkowski@ece.arizona.edu).

Color versions of one or more of the figures in this letter are available online at http://ieeexplore.ieee.org.

Digital Object Identifier 10.1109/LAWP.2010.2051311

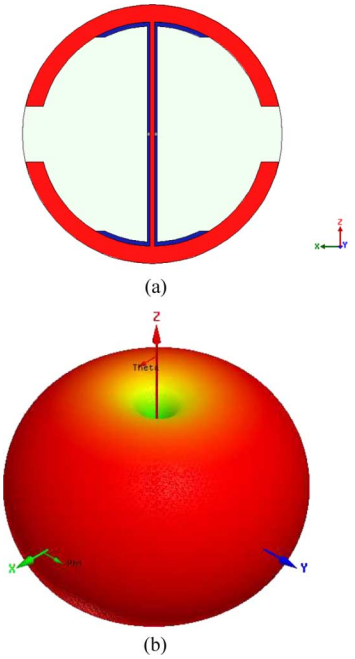

Fig. 1. Electrically small planar electric dipole. (a) Electric dipole structure with outer radius of 15 mm. (b) HFSS-predicted 3D directivity pattern at $f_{\rm res} = 1.5628$GHz. The maximum directivity is 1.911 dB in the xy plane.

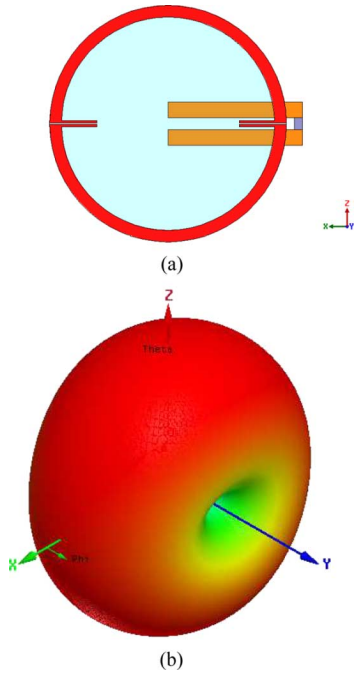

Fig. 2. Electrically small planar magnetic dipole. (a) Magnetic dipole (CLL) structure with outer radius of 15 mm. (b) HFSS-predicted 3D directivity pattern at $f_{\rm res} = 1.5739$ GHz. The maximum directivity is 1.907 dB in the xz plane.

long. Their vertical legs are respectively 0.5 and 1.2 mm wide. In the HFSS simulations, the center-fed gap of the driven dipole is a lumped port source that is 0.4 mm long. The HFSS-predicted $|S_{11}|$ values reach their lowest value in the 1–2 GHz range, -33 dB, at the resonance frequency $f_{\rm res} = 1.5628$ GHz with an overall efficiency (OE) equal to 90%, i.e., $OE(f_{\rm res}) = (1 - |S_{11}(f_{\rm res})|^2) \times RE(f_{\rm res})$, where $RE(f_{\rm res})$ is its radiation efficiency at $f_{\rm res}$. The 10-dB bandwidth is $BW_{10\ \rm dB} = 24.6$ MHz. Consequently, the ka value of this antenna at $f_{\rm res}$ is 0.491, where a is the radius of the smallest enclosing sphere of the entire antenna system and the wavenumber $k = 2\pi/\lambda_{\rm res}$, $\lambda_{\rm res}$ being the free-space wavelength at $f_{\rm res}$. This value is smaller by more than half of the maximum value allowed for the antenna to be electrically small, this maximum being defined by the corresponding radiansphere radius $a_{\max} = 1/k = \lambda_{\rm res}/(2\pi)$. From its half-power VSWR frequencies, the Q value of this antenna at $f_{\rm res}$ is 44.304, which, in comparison to the corresponding lower bound $Q_{\rm lb} = RE \times [1/(ka)^3 + 1/(ka)]$ [13], gives the $Q_{\rm ratio} = Q/Q_{\rm lb} = 4.23$. The HFSS-predicted 3D directivity pattern at $f_{\rm res}$ given in Fig. 1(b) clearly shows that this ESA acts as an electric dipole oriented along the z-axis.

Electrically small magnetic dipole antennas have been achieved with similar performance characteristics [8]. In those designs, the NFRP elements are capacitively loaded loops (CLLs) that are electrically coupled to the driven monopole, which is coaxially fed through a finite ground plane. Based on those protractor antenna concepts, the no-ground-plane, 2-oz, 31-mil Rogers Duroid 5880 board material design shown in Fig. 2(a) is proposed. Two half-moon-shaped CLLs located on one side of the Duroid sheet are electrically coupled to the driven electrically small, coplanar stripline (CPS)-fed dipole antenna located on the other side. The outer radii of the CLL elements are 15.0 mm; their outer traces are 2.0 mm wide. There is a 0.2-mm gap between their legs, which are 0.3 mm wide and start at 5.0 mm from the origin of the CLLs, the y-axis. The CPS feedlines are 2.0 mm wide and are 17.0 mm long starting from the y-axis, i.e., there is a 2.0-mm extension beyond the outer radius of the CLL elements across which the HFSS lumped port source is connected. The distance between them (the gap) is 1.5 mm. The HFSS-predicted $|S_{11}|$ values reach their lowest value in the 1–2 GHz range, -30 dB, at the resonance frequency $f_{\rm res} = 1.5739$ GHz with $OE = 91\%$ and $BW_{10\ \rm dB} = 25.1$ MHz. Consequently, the ka value at $f_{\rm res}$ is 0.4945. The quality factor $Q = 73.42$ and, hence, $Q_{\rm ratio} = 7.14$ at $f_{\rm res}$. Because the electric fields generated by the currents on the CPS-fed dipole drive the currents on the CLLs in an offset configuration, the associated loop mode dominates the radiation process [8]. Consequently, as the HFSS-predicted 3D directivity pattern at $f_{\rm res}$ given in Fig. 2(b) clearly shows, this ESA acts as a magnetic dipole oriented along the y-axis.

III. Huygens Source

These electrically small, Duroid-based, planar electric and magnetic NFRP dipole antennas are combined to achieve the desired Huygens source with only a single feed structure. Their dimensions are adjusted to produce the radiated field amplitudes that realize the desired Huygens source behavior while maintaining a nearly complete match to the 50-Ω source. Two combinations are proposed. One is the 3D structure shown in Fig. 3(a); the second is the planar structure shown in Fig. 4(a). While the planar version is a more realizable design, both are given to illustrate the possible driving mechanisms and orientations of the two individual component antennas.

The electric and magnetic dipolar NFRP elements in the 3D version, Fig. 3(a), are orthogonal and are both centered at the

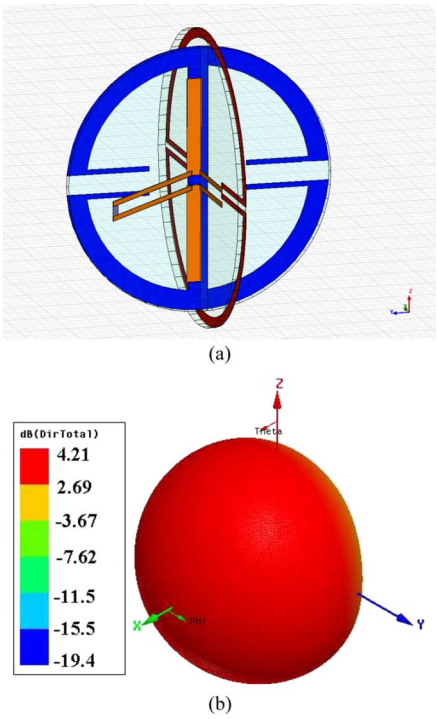

Fig. 3. Electrically small sphere Huygens source. (a) Structure with outer radius of 15 mm. (b) HFSS-predicted 3D directivity pattern at $f_{\rm res} = 1.5395$ GHz.

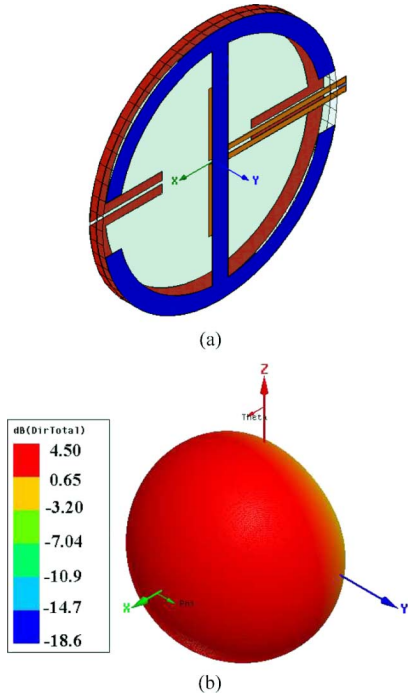

Fig. 4. Electrically small planar Huygens source. (a) Structure with outer radius of 15 mm. (b) HFSS-predicted 3D directivity pattern at $f_{\rm res} = 1.475$ GHz.

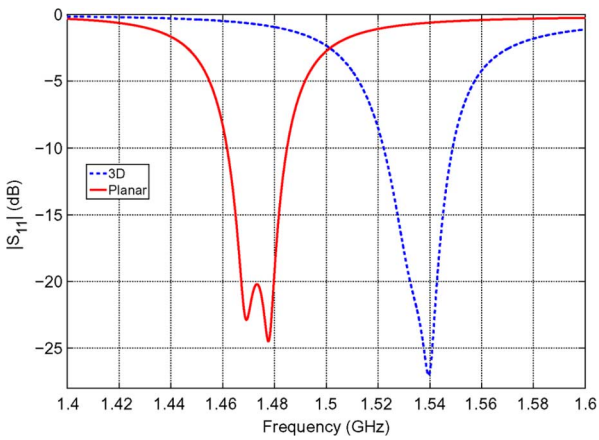

Fig. 5. HFSS-predicted $|S_{11}|$ values versus frequency for the electrically small Huygens sources.

origin. The planar electric NFRP element lies in the yz plane; it produces an electric dipole field relative to the z-axis. Its top arc is 2.0 mm wide; its leg width is 2.0 mm. Its outer radius has been decreased to 13.0 mm to accommodate the presence of the magnetic NFRP element in the 3D configuration. If no other variations were made, its resonance frequency would naturally be higher than the original value. Consequently, the legs shown in Fig. 3(a) were included on it. They are oriented parallel to the x-axis and start at 5.0 mm from the z-axis. Their width is 0.5 mm, and the gap between them is 2.0 mm. The additional capacitance they produce lowers the resulting resonance frequency to the desired value. The electric NFRP element is electrically coupled to a driven printed dipole that lies on the backside of the same Duroid sheet and is oriented and centered along the z-axis. This driven electric dipole has a width of 1.5 mm and an arm length of 9.90 mm.

The planar magnetic NFRP element lies in the xz plane on a second Duroid sheet. Its CLLs produce a magnetic dipole field relative to the y-axis. These CLLs have an outer radius of 15.0 mm and a 1.0-mm trace width. Their legs start at 5.9 mm from the z-axis and are 0.5 mm wide. The gap between them is 0.6 mm. The magnetic NFRP element is also electrically coupled to the driven elements by introducing another pair of legs that lie on the backside of the same Duroid sheet and are connected to the printed dipole on the other sheet as shown in Fig. 3(a). These legs are oriented parallel to the $-$x-axis; they start at 9.0 mm from the z-axis and have 0.5-mm widths. The electric dipole is fed directly by a coplanar stripline, which lies in the plane oriented 45° with respect to both the $-$x and $+$y axes. This CPS feedline extends out to 17.0 mm from the z-axis; it is parallel to and symmetric about the xy plane. Its trace width and gap are 0.5 and 1.0 mm, respectively. Consequently, the printed dipole's feed gap is 1.0 mm. This CPS feedline is excited in the HFSS simulations with a lumped port source that is located across its 2.0-mm extension beyond the outer radius of the CLL elements.

The HFSS-predicted $|S_{11}|$ values are shown in Fig. 5. At the resonance frequency $f_{\rm res} = 1.5395$ GHz, one finds $|S_{11}| = -27$ dB, $RE = 84.27\%$, $OE = 84.12\%$, and $BW_{10\,\rm dB} = 26.6$ MHz. Consequently, the ka value of this antenna at $f_{\rm res}$ is 0.484. The HFSS-predicted 3D directivity pattern at $f_{\rm res}$ is given in Fig. 3(b). Its maximum directivity is 4.21 dB along the x-axis, while its minimum, -19 dB, is along the $-$x-axis, which gives a 23.2-dB front-to-back ratio. Taking into account the overall efficiency, the maximum realized gain is 3.47 dB. These results

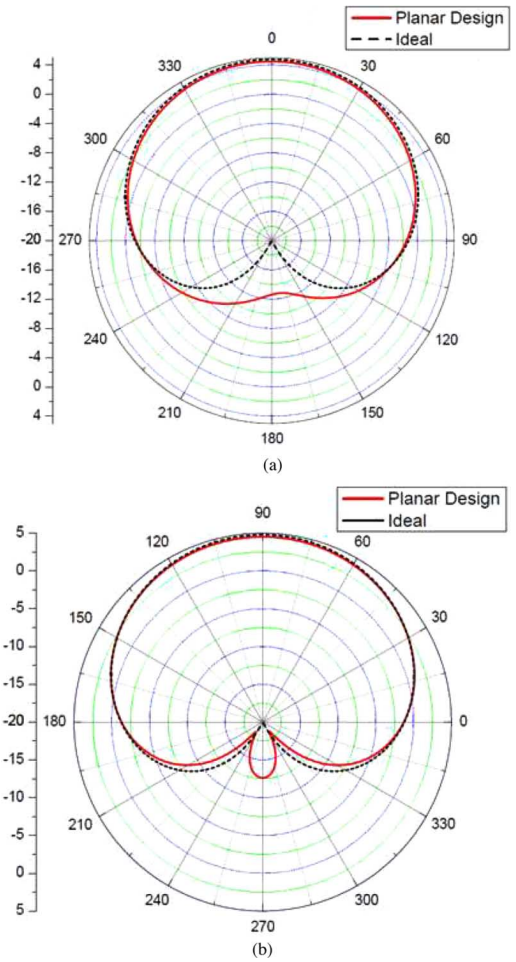

Fig. 6. Planar Huygens source directivity patterns at $f_{\rm res} = 1.475$ GHz. (a) E-plane. (b) H-plane.

demonstrate that the antenna in Fig. 3 is a well-matched, electrically small Huygens source. We note that although this is a spherical structure, whose phase centers of the electric and magnetic dipoles are collocated, the feeding structure would be very difficult to implement, and the size of the electrical dipole is limited by the magnetic dipole, making the amplitude matching challenging. A series of simulations have suggested that the nonplanar nature of the NFRP elements and the CPS feedline limit the maximum directivity of this configuration to approximately the best value reported here. Also note that the $|S_{11}|$ values shown in Fig. 5(a) clearly indicate the presence of two nearby resonances. As a result, the bandwidth is reported rather than a non-well-defined Q value [14].

The planar design shown in Fig. 4(a) overcomes the noted shortcomings in the 3D design. The planar design is a three-metal, two-dielectric-layer structure. It is constructed as a two-piece stack of the 2-oz, 31-mil Rogers Duriod 5880 board material. The electric NFRP element is parallel to the xz plane, oriented along the z-axis, and lies on the outside of one Duroid sheet. It produces an electric dipole field relative to the z-axis. The magnetic NFRP element is parallel to the xz plane and lies on the outside of the other Duroid sheet. Its legs are oriented along and symmetrically located about the x-axis. It produces a magnetic dipole field relative to the y-axis. The directly driven printed electric dipole element and its CPS feedline constitute the middle metal layer. The printed dipole is oriented along the z-axis; its arms electrically couple to the electric NFRP element. The CPS feedline is oriented along and symmetrically located about the $-$x-axis. It electrically couples directly to the magnetic NFRP element. The printed driven dipole is 1.2 mm wide and has an arm length of 7.97 mm. The CPS feedline has 0.611-mm-wide traces with a 0.4-mm gap between them; it starts at 17.0 mm from the z-axis. For the HFSS simulations, a lumped port source is again located on the 2.0-mm extension of this CPS structure beyond the outer radii of the NFRP dipole elements. Both the electric and magnetic NFRP elements have a 15.0-mm outer radius. The top arc and the legs of the electric NFRP element are 2.0 mm wide. Its gaps are 6.0 mm long. The magnetic NFRP element has a 2.0-mm trace width. Its legs start at 5.7 mm from the origin of the CLLs, the y-axis, and are 1.0 mm wide. There is a 0.4-mm gap between them.

The HFSS-predicted $|S_{11}|$ values are shown in Fig. 5. They even more clearly corroborate the presence of the two nearby resonances from the electric and magnetic NFRP elements. At the resonance frequency of the antenna $f_{\rm res} = 1.475$ GHz, one has $|S_{11}| = -21.1$ dB, $RE = 86.58\%$, $OE = 85.91\%$, and $BW_{10\ \rm dB} = 23.2$ MHz. Consequently, the ka value of this antenna at $f_{\rm res}$ is 0.463. As with the 3D version, the HFSS simulations of this planar Huygens source show the currents on the NFRP elements dominate the radiation process rather than those on the driven elements. They also show that this planar version has a higher maximum directivity and a marginally higher radiation efficiency than the 3D version. The HFSS-predicted 3D directivity pattern at $f_{\rm res}$ of this ESA is given in Fig. 3(c). Its directivity along the $+$x-axis, 4.50 dB, is its maximum, while along the $-$x-axis it is -12.63 dB, which gives a 17.1-dB front-to-back ratio. Taking into account the overall efficiency, the maximum realized gain is 3.87 dB.

To illustrate the differences between the proposed planar Huygens source and the ideal one, their HFSS-predicted E-plane and H-plane directivity patterns at $f_{\rm res}$ are compared in Fig. 6. The ideal results are obtained from the analytical model of an infinitesimal electric dipole oriented along the z-axis and collocated with an infinitesimal magnetic dipole oriented along the y-axis. These pattern results clearly show that the proposed planar Huygens source has directivity performance characteristics that are again very close to the ideal Huygens source. The most deviation from ideal occurs in the backlobe directions. There are several factors that contribute to this performance deviation from the ideal Huygens source. The incorporation of the realistic feed structure into the planar Huygens source model has a modest impact on the directivity patterns because the currents on the CPS feedline are in opposite directions. In the configuration shown in Fig. 4(a), the loop and dipole are located at slightly different locations. The distance between them is 62 mil or $\lambda/129$. As noted above, this phase center distance is zero in the ideal Huygens source; its nonzero value in the realistic configuration also has an impact on the directivity patterns. Finally, because the ideal Huygens source requires the same amplitude of the electric and magnetic dipole patterns, and because this is very difficult to achieve in any design, slight

variations in these amplitudes exist. These variations are the dominant factor in the directivity deviation from the ideal value.

IV. Conclusion

In this letter, both electrically small electric and magnetic dipoles that have high radiation efficiencies and are nearly completely matched to a 50-Ω source were introduced. They both are near-field resonant parasitic designs; their NFRP elements are electrically coupled to their driven electric dipole sources. Based on their individual feeding mechanisms, orthogonally radiating versions of these electric and magnetic dipole antennas were combined together to form an electrically small Huygens source with a single feedline structure.

Both the reported spherical and planar Huygens sources show directivity patterns that are close to those of the ideal Huygens source. Both were shown to have high radiation efficiencies and were nearly completely matched to a 50-Ω source. Although it was found that the spherical Huygens source deviates slightly further from the ideal directivity performance than does the planar version, it theoretically has the potential to be able to approach the ideal limit more closely because the phase centers of its two dipoles coincide while those of the planar version are very slightly offset. Nonetheless, the practical realization of either case requires some form of feeding structure and equality of the field amplitudes generated by both dipoles. These will be the eventual limiting factors to reaching the ideal directivity performance of a Huygens source.

References

[1] S. R. Best, "The radiation properties of electrically small folded spherical helix antennas," *IEEE Trans. Antennas Propag.*, vol. 52, no. 4, pp. 953–960, Apr. 2004.

[2] P. Jin and R. W. Ziolkowski, "Low Q, electrically small, efficient near field resonant parasitic antennas," *IEEE Trans. Antennas Propag.*, vol. 57, no. 9, pp. 2548–2563, Sep. 2009.

[3] H. Mosallaei and K. Sarabandi, "Antenna miniaturization and bandwidth enhancement using a reactive impedance substrate," *IEEE Trans. Antennas Propag.*, vol. 52, no. 9, pp. 2403–2414, Sep. 2004.

[4] A. D. Yaghjian, T. H. O'Donnell, E. E. Altshuler, and S. R. Best, "Electrically small supergain endfire arrays," *Radio Sci.*, vol. 43, p. RS3002, May 2008.

[5] A. D. Yaghjian, "Increasing the supergain of electrically small antennas using metamaterials," in *Proc. EuCAP*, Apr. 2009, pp. 858–860.

[6] G. Mumcu, K. Sertel, and J. L. Volakis, "Miniature antenna using printed coupled lines emulating degenerate band edge crystals," *IEEE Trans. Antennas Propag*, vol. 57, no. 6, pp. 1618–1624, Jun. 2009.

[7] P. Jin and R. W. Ziolkowski, "Broadband, efficient, electrically small metamaterial-inspired antennas facilitated by active near-field resonant parasitic elements," *IEEE Trans. Antennas Propag.*, vol. 58, no. 2, pp. 318–327, Feb. 2010.

[8] P. Jin and R. W. Ziolkowski, "Multi-frequency, linear and circular polarized, metamaterial-inspired near-field resonant parasitic antennas," *IEEE Trans. Antennas Propag.*, Oct. 2009, submitted for publication.

[9] A. W. Love, "Some highlights in reflector antenna development," *Radio Sci.*, vol. 11, pp. 671–684, Aug.–Sep. 1976.

[10] S. R. Best, "Progress in the design and realization of an electrically small Huygens source," presented at the iWAT, Lisbon, Portugal, Mar. 1–3, 2010, paper SS4.4.

[11] S. R. Best, "A low Q electrically small magnetic (TE mode) dipole," *IEEE Antennas Wireless Propag. Lett.*, vol. 8, pp. 572–575, 2009.

[12] P. Jin and R. W. Ziolkowski, "Multiband extensions of the electrically small near field resonant parasitic Z antenna," *IET Proc. Microw., Antennas Propag.*, 2010, to be published.

[13] A. D. Yaghjian and S. R. Best, "Impedance, bandwidth, and Q of antennas," *IEEE Trans. Antennas Propag.*, vol. 53, no. 4, pp. 1298–1324, Apr. 2005.

[14] H. R. Stuart, S. R. Best, and A. D. Yaghjian, "Limitations in relating quality factor to bandwidth in a double resonance small antenna," *IEEE Antennas Wireless Propag. Lett.*, vol. 6, pp. 460–463, 2007.